Langmuir

Article

pubs.acs.org/Langmuir

Visible-Light Photoconversion of Carbon Dioxide into Organic Acids in an Aqueous Solution of Carbon Dots

Sushant Sahu,[†] Yamin Liu,[†] Ping Wang,[†] Christopher E. Bunker,*[,‡] K. A. Shiral Fernando,[§] William K. Lewis,[§] Elena A. Guliants,[§] Fan Yang,[†] Jinping Wang,[†] and Ya-Ping Sun*[,†]

[†]Department of Chemistry and Laboratory for Emerging Materials and Technology, Clemson University, Clemson, South Carolina 29634, United States

[‡]Air Force Research Laboratory, Propulsion Directorate, Wright-Patterson Air Force Base, Dayton, Ohio 45433, United States

[§]University of Dayton Research Institute, Sensors Technology Office, Dayton, Ohio 45469, United States

ABSTRACT: Carbon "quantum" dots (or carbon dots) have emerged as a new class of optical nanomaterials. Beyond the widely reported bright fluorescence emissions in carbon dots, their excellent photoinduced redox properties that resemble those found in conventional semiconductor nanostructures are equally valuable, with photon−electron conversion applications from photovoltaics to CO_2 photocatalytic reduction. In this work we used gold-doped carbon dots from controlled synthesis as water-soluble catalysts for a closer examination of the visible-light photoconversion of CO_2 into small organic acids, including acetic acid (for which the reduction requires many more electrons than that for formic acid) and, more interestingly, for the significantly enhanced photoconversion with higher CO_2 pressures over an aqueous solution of the photocatalysts. The results demonstrate the nanoscale semiconductor-equivalent nature of carbon dots, with excellent potential in energy conversion applications.

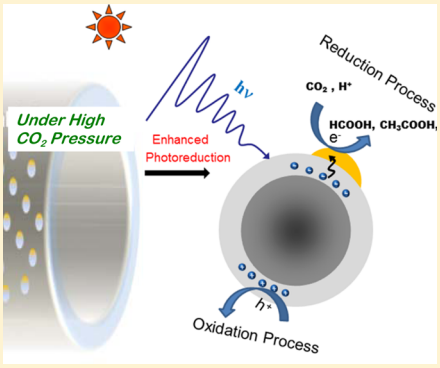

INTRODUCTION

The level of carbon dioxide (CO_2) in the atmosphere and its significant environmental implications have generated much concern, promoting the development of various carbon sequestration strategies. Photocatalytic conversion is obviously a compelling approach in this regard, in which CO_2 is reduced back to hydrocarbon fuels. Even more desirable is the use of solar energy for the photoreduction, which presents a major challenge for the effective photon harvesting by the catalysts across the solar spectrum.[1,2] Among widely employed photocatalysts for the purpose of CO_2 reduction have been nanoscale wide-bandgap semiconductors such as titanium dioxide (TiO_2) and cadmium sulfide (CdS) nanoparticles.[1−4] However, as limited by their bandgap transitions, these nanomaterials are generally ineffective in harvesting visible photons over a broad spectral range. Thus, various enhancement approaches including the use of doped TiO_2 nanotubes and/or dye sensitization to extend the absorption of the photocatalysts into the visible have been developed, with some significant successes. For example, Feng et al. prepared TiO_2 nanotube arrays via the anodic oxidation of titanium foil in an electrolyte.[5] The arrays under sunlight could catalyze the reduction of CO_2 into methane, and the reduction efficiency could be enhanced substantially after the arrays were "coated" with ultrafine platinum nanoparticles.[5] Woolerton et al. used enzyme-modified TiO_2 nanoparticles (Degussa P25) with a ruthenium bipyridyl complex as a visible-light photosensitizer for the CO_2 photoconversion.[6] Asi et al. synthesized a nanocomposite of TiO_2 with silver bromide for the visible-light (420 nm and longer) photoreduction of CO_2.[7]

More recently, Cao et al. took a rather different approach to using surface-functionalized small carbon nanoparticles, dubbed "carbon dots" (Figure 1),[8,9] for the absorption of visible photons to drive photocatalytic processes.[10] In the photoreduction of CO_2, the carbon dots were surface-doped with a

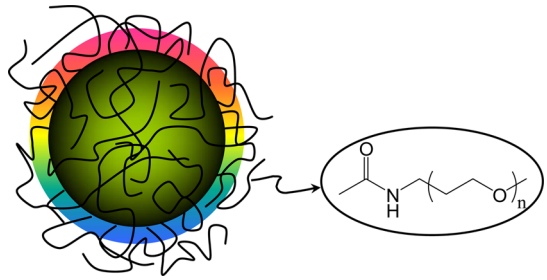

Figure 1. Cartoon illustration of the PEG_{1500N}-functionalized carbon dot, with the rainbow-colored "shell" signifying that the fluorescence is from the passivated surface of the dot. The shell illustration does not imply a true core−shell structure for the carbon dot, as the passivation molecules covering the carbon particle surface likely form a structurally random soft layer that is significantly different from the kind of shell found in conventional semiconductor QDs.

Received: March 19, 2014
Revised: June 4, 2014
Published: June 27, 2014

   dx.doi.org/10.1021/la5010209 | *Langmuir* 2014, 30, 8631−8636

small amount of gold or platinum metal, which was designed to concentrate the photogenerated electrons, similar to what was widely practiced in the development of conventional nanoscale semiconductor-based photocatalysts.[4] The photocatalytic conversion of CO_2 was probed by quantifying the formation of formic acid as a significant product,[10] from which the estimated quantum yields for the photoreduction were substantial in reference to those achieved in the literature with the use of semiconductor nanoparticles as photocatalysts.[3,4,10] More importantly in terms of a primary purpose in that study to understand the photoexcited state processes in small carbon nanoparticles,[10] the photocatalytic reduction results served to confirm the presence of photoinduced charge separation in carbon dots, as already suggested by the fluorescence quenching results of carbon dots with either electron donors or acceptors.[9,11]

Beyond mechanistic implications (with some other carbon-based photocatalytic systems[12−14]), the previous study opened the possibility for carbon dots to serve as a new platform of potent photocatalysts for more efficient CO_2 photoreduction. However, because it is a new platform, there is naturally the demand for more experimental results for further validation. In the work reported here, we used gold-doped carbon dots from better-controlled synthesis as aqueous soluble catalysts for a closer examination of the visible-light photoconversion of CO_2 into small organic acids, including acetic acid (whose formation requires many more electrons than that of formic acid),[15] and more interestingly for the significantly enhanced photoconversion with higher CO_2 pressures over an aqueous solution of the catalysts. The results from the pressure-dependent (and thus CO_2 concentration-dependent) study under otherwise the same experimental conditions are particularly valuable in terms of confirming the participation of CO_2 in the reaction as the source of the converted organic acids and also the photocatalytic functions of the carbon dots.

RESULTS AND DISCUSSION

The photocatalytic reactions were carried out in aqueous solutions under pressurized CO_2 conditions. In the catalyst preparation, the fluorescent carbon dots with the core carbon nanoparticles functionalized by oligomeric poly(ethylene glycol) diamine (PEG_{1500N}, Figure 1) were synthesized under more controlled conditions (primarily more precise temperature control in the functionalization reaction) for more effective carbon particle surface passivation and the associated bright fluorescence emissions, as reported previously.[16] These carbon dots in aqueous solution exhibited fluorescence quantum yields of around 20% at 400−450 nm excitation, comparable to or better than what were observed in other batches of similarly synthesized PEGylated carbon dots in previous studies.[16] For the photochemical doping of the carbon dots by gold metal, the aqueous solution of the carbon dots was irradiated in the presence of gold salt $HAuCl_4$, where the electrons from the photoinduced charge separation in the carbon dots were likely responsible for the reductive formation of gold metal (Figure 2).[17,18] Since the radiative recombination of the surface-confined electrons and holes is believed to be responsible for the observed fluorescence emission in carbon dots,[9] the metal doping was accompanied by rapidly diminishing fluorescence intensities in the solution (Figure 2), as expected.[17]

The doping level of gold on carbon dots was monitored by the emergence of the gold plasmon band in optical absorption

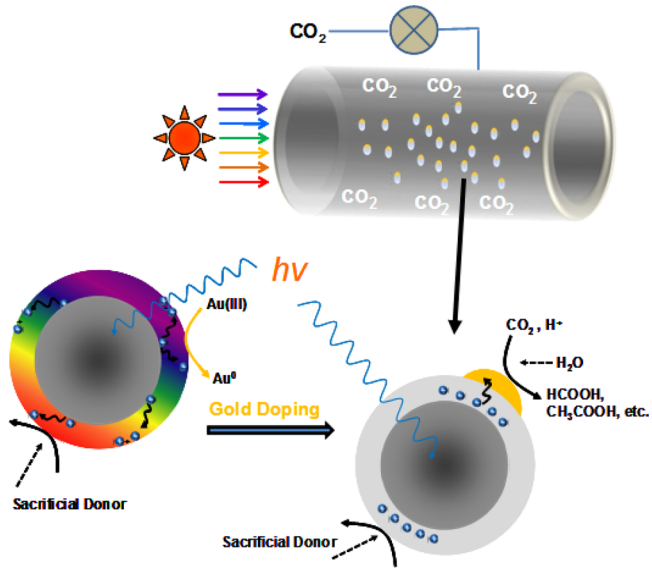

Figure 2. Cartoon illustrations of (upper) the high-pressure optical reactor. (Lower left) Photoreductive doping of the carbon dot with gold, completely quenching the dot-surface-based fluorescence (illustrated as the change in the dot surface from rainbow to gray) and (lower right) the gold-doped carbon dot as a photocatalyst for CO_2 conversion, where the doped gold (in yellow) was small in quantity, insufficient to form a shell, and likely random in terms of size and shape. The sacrificial electron donor was isopropanol added in some experiments or PEG_{1500N} molecules on the surface of the carbon dots in the absence of isopropanol.

spectra (Figure 3). The association of the nanoscale gold and carbon dots, namely, the doping, could be confirmed directly by the transmission electron microscopy (TEM) imaging comparatively in both transmission and *Z*-contrast modes (Figure 3) and also indirectly by the observed complete fluorescence quenching due to the doped gold interfering with the emissive processes in carbon dots (Figure 2).[17] The gold-doped carbon dots used as photocatalysts in this study generally had a gold-to-carbon (in the nanoparticle core) molar ratio of around 1:100.

The photocatalytic reduction of CO_2 in an aqueous solution of the gold-doped carbon dots was carried out at ambient temperature (25 °C) in high-pressure cylindrical optical cells (Figure 2) capable of taking the CO_2 pressure up to at least 2000 psia, corresponding to an aqueous CO_2 concentration of up to 1.37 M (calculated according to data available in the literature).[19] Small organic acids in the reaction mixture were targeted for detection and analysis quantitatively. The acids were harvested by distilling the reaction mixture into a basic aqueous solution (pH ∼11), followed by recovering the salts thus formed for NMR characterization and other analyses.

The ^1H and ^{13}C NMR results suggested a substantial presence of formic acid as a significant product of the CO_2 photoreduction, as generally known in the literature,[4,20−24] and also acetic acid.[15,25−30] Separately, the solution used in the NMR measurements was acidified (pH ∼3) to convert the salts to corresponding acids for GC-MS analyses, from which the results also identified formic acid and acetic acid, as expected.

In the literature,[15,25−30] acetic acid has been identified as a product in CO_2 photoreduction with the use of other photocatalysts, though quantity-wise from minor to negligible in almost all studies. Therefore, since the photocatalytic activities of carbon dots are due to the photochemical processes

dx.doi.org/10.1021/la5010209 | *Langmuir* 2014, 30, 8631−8636

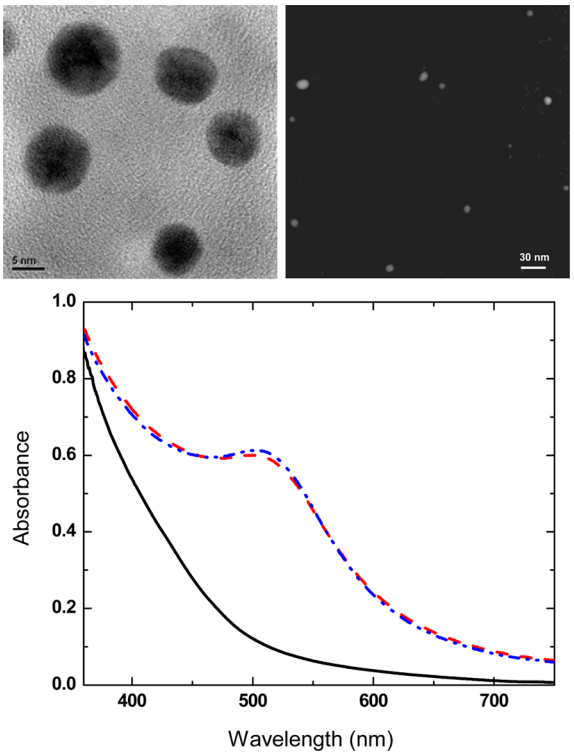

Figure 3. (Upper) TEM images of the gold-doped carbon dots (left, in transmission mode; right, in *Z*-contrast mode, where *Z* refers to the atomic number so that the contribution of the doped gold is emphasized). (Lower) Optical absorption spectra of the carbon dots without (−) and with gold (−−) and recovered postreaction (−···−).

in the core carbon nanoparticles, the concern was the potential involvement of the carbon in the core as a source of carbon atoms in the observed acetic acid. In control experiments, ^{13}C-labeled CO_2 ($NaH^{13}CO_3$ with 99% ^{13}C as a source) was used in the same photoreduction reactions. The ^{13}C NMR results for the formic acid and acetic acid suggested major enhancement effects in both, with the corresponding ^{13}C NMR signals readily detected in many fewer scans than what was required for samples without the ^{13}C enrichment, due to the products from ^{13}C-labeled CO_2 (or, more specifically, $H^{13}COOH$ and $^{13}CH_3{}^{13}COOH$).

Other experimental evidence against any potential involvement of the carbon atoms in carbon dots included the observation that the use of the same carbon dots without a gold coating for the photocatalytic conversion of CO_2 resulted in much lower yields for both formic acid and acetic acid. Mechanistically, it is believed that the photoexcitation of carbon dots results in efficient charge separation, with the generated electrons and holes trapped at surface sites on the carbon dots. The electrons and holes would otherwise recombine radiatively for the fluorescence emission in carbon dots, but the metal doping interrupted the radiative recombination by scavenging the electrons (Figure 2).[9,17] Here the doped gold could apparently harvest and concentrate the photogenerated electrons in the carbon dots, thus more effectively in the photocatalytic activities for the CO_2 reduction, as generally understood in the literature.[2,4]

In a further examination of the involvement of water as a source of hydrogen in the formed organic acids, the photocatalytic reduction of CO_2 was performed in a deuterated water solution under the same experimental conditions, followed by the same product collection and isolation procedures. In the subsequent ^{2}H NMR characterization (regular water as the solvent), the expected $DCOO^-$ and CD_3COO^- NMR signals could readily be detected at 8.47 and 1.89 ppm, respectively, suggesting the participation of D_2O in the photoreduction. A mechanism known in the literature in which the involvement of water in the photocatalytic conversion of CO_2 might be associated with a two-step reduction process, first the photocatalytic splitting of water for atomic hydrogen and then the addition of hydrogen to CO_2.[3,31] The observed deuteration of both formic acid and acetic acid from the reaction in D_2O is consistent with such a mechanism and also reaffirms the mechanistic connection between the formation of the two organic acids in the photocatalytic reduction of CO_2.

There are several ways to evaluate the performance of catalysts in the CO_2 photoreduction reaction,[4] among which a more popular one has been the *R* value measuring the amount of products produced per hour of light illumination for a specific amount of photocatalyst

$$R = \frac{W_P}{tW_C} \quad (1)$$

where W_P is the amount of photoproducts in millimoles (mmol), t is the photoirradition time in hours (h), and W_C is the amount of photocatalyst used in grams (g). For the gold-doped carbon dots as photocatalysts in this work, quantitatively the amounts of the small organic acids produced in the photoreduction were subject to some variations with experimental conditions such as different batches or quantities of catalysts and reactor setups, which also affected the relative populations of the two acids in the reaction mixtures. Nevertheless, with the short-path optical cell as a high-pressure photoreactor under a specifically controlled condition (CO_2 pressure of 700 psia and photoirradiation in the 405−720 nm wavelength range for 4 h), the observed *R* values for formic acid and acetic acid were 1.2 and 0.06 mmol h^{-1} g^{-1}, respectively. The performance of the former compares favorably to what has been reported in the literature for other photocatalysts. For example, in the study by Zhao et al. on CO_2 photoreduction with the cobalt phthalocyanine−TiO_2 nanocomposite as the photocatalyst and visible-light irradiation, the best *R* value for formic acid was about 0.15 mmol $h^{-1}g^{-1}$.[22] Johne and Kisch used ZnS nanoparticles loaded on a silica matrix as photocatalysts for CO_2 reduction with 2,5-dihydrofuran as a reducing agent and UV-light irradition, achieving a formate production rate of about 0.29 mmol/h (or approximately 0.6 mmol $h^{-1}g^{-1}$ in terms of the *R* value).[21]

The significant acetic acid production with the use of gold-doped carbon dots as photocatalysts is somewhat unique, as this is generally a very minor product in the CO_2 photoreduction with other catalysts.[15,25−30] The previously highest *R* value for acetic acid in the literature was from the work of Pathak et al., where well-dispersed TiO_2 nanoparticles were used as photocatalysts for UV-light reduction in supercritical CO_2 under high pressure, though the estimated *R* value was still rather small (on the order of 0.006 mmol h^{-1} g^{-1}).[28] Irvine et al. also observed a significant amount of acetic acid in their colloidal CdS-based photocatalytic CO_2 reduction in aqueous $NaHCO_3$ with sulfite or hydroquinone as a hole acceptor (320−580 nm photoirradiation), with an estimated acetic acid production rate of about 0.00125 mM/h (or an *R* value of

dx.doi.org/10.1021/la5010209 | *Langmuir* 2014, 30, 8631−8636

about 0.004 mmol h^{-1} g^{-1}).[26] The relatively more efficient formation of acetic acid in the work reported here reflects upon the effectiveness of the gold-doped carbon dots as photocatalysts for visible-light-driven CO_2 conversion, as the reduction to acetic acid requires overall eight electrons, regardless of any detailed mechanisms.[15]

$$2CO_2 + 8H^+ + 8e^- \rightarrow CH_3COOH + 2H_2O \quad (2)$$

Again in studies already reported in the literature,[15,25−30] acetic acid has generally been a very minor or negligible product in CO_2 photoconversion. Therefore, the formation mechanism for the product is poorly understood, except for a general acknowledgment of the mechanistic complexity. Among the three proposed mechanisms in the literature,[4,26,29,32] two assumed the dimerization of initially reduction-generated radical or radical anion species as a key step in the formation of acetic acid, specifically, OHC· or CO_2^{-}· dimerized to OHC−CHO or $^{-}$OOC−COO^{-}, respectively, followed by further photoreduction.[26,32] The other mechanism in the acetic acid formation called for the reductive coupling of methanol and ·COOH, both of which are from initial steps in the CO_2 photoreduction process.[29] A common theme is that acetic acid shares intermediates with formic acid and/or reacts further from the latter, signifying the important role of formic acid in the understanding of the photocatalytic CO_2 conversion.

For a more systematic evaluation of the photoconversion under different CO_2 pressures, the reactions were carried out in the long-path high-pressure optical cell (thus a larger reactor volume for more samples/product quantities and thus relatively improved accuracy) under otherwise the same experimental conditions for all CO_2 pressures. The formic acid production obviously increased with the increasing CO_2 pressure (Figure 4), mainly because the CO_2 concentration in aqueous solution

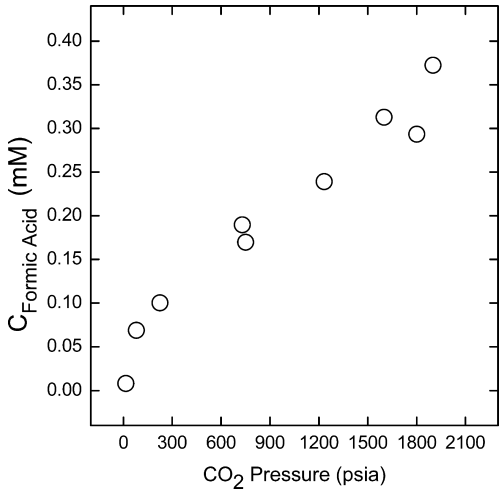

Figure 4. Results in terms of formic acid concentrations in the reaction mixtures from a series of photoconversion reactions in aqueous solutions of the carbon dots under different CO_2 pressures (in the long-path optical cell as the high-pressure reactor).

increases with increasing pressure. At 1900 psia, the amount of formic acid was about an order of magnitude higher than that produced under ambient CO_2 pressure, which should correspond roughly to the same magnitude of increase in the photocatalytic reaction quantum yield for the formic acid formation (around 0.3% in the CO_2-saturated aqueous solution under ambient pressure,[10] estimated by using the method of Mallouk and coworkers[33,34]). The strong CO_2 pressure dependence might be understood in terms of the importance of the initial interactions between the photoexcited catalysts and CO_2 molecules in the conversion to formic acid, with more CO_2 molecules in the aqueous solution under a higher CO_2 pressure in the optical cell and/or the involvement of more complex multistep processes in the photoconversion reaction. Shown in Figure 5 is a comparison of the R values for formic acid and acetic acid from the experiments at different CO_2 pressures.

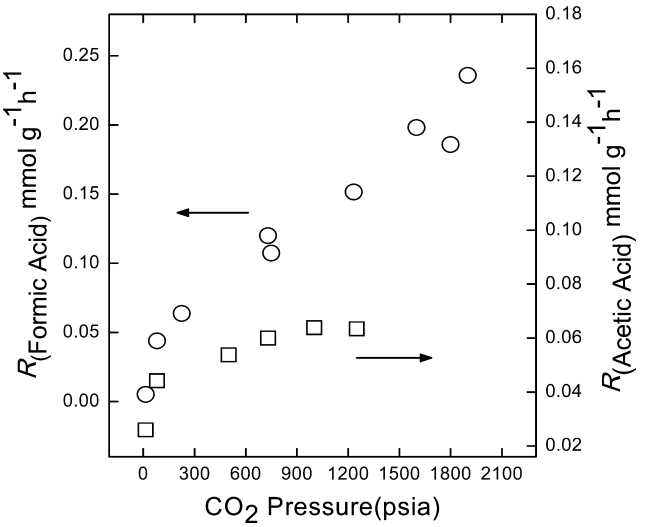

Figure 5. Comparison of R values for the photoconversion to formic acid (o) and acetic acid (□) in reactions under different CO_2 pressures.

The gold-doped carbon dots as photocatalysts were apparently stable in terms of their optical properties and catalytic activities. For example, upon continued photoirradiation for 6 h or longer in the photocatalytic reaction for CO_2 conversion, the optical absorption spectrum of the photocatalysts postreaction exhibited no significant changes from that prereaction (Figure 3). The photocatalysts could also be recovered from the reaction mixtures and reused in the subsequent photoreduction reactions of CO_2. The difference between the use of new and recovered photocatalysts is generally within the typical experimental variation (the changes in the results with the use of new catalysts in several experiments under the same conditions).

In summary, carbon dots with a gold coating and thus diminished fluorescence emission are potent photocatalysts for the conversion of CO_2 to small organic acids. The formation of a significant amount of acetic acid, which requires many electrons in the photoreduction, reflects upon the effectiveness of the carbon dots as photocatalysts. The photocatalytic functions are apparently not limited to the carbon dots synthesized in this study, as even those prepared with carbon soot from overcooked barbequed meat exhibited similar activities.[35] The substantially enhanced photoconversion in aqueous solution of the catalysts under higher CO_2 pressures is not only important mechanistically, suggesting the role of the CO_2 concentration in the harvesting of photogenerated electrons and thus the photoconversion quantum yield, but also valuable technologically, with pressurized CO_2 as a more

dx.doi.org/10.1021/la5010209 | Langmuir 2014, 30, 8631−8636

favorable reaction condition for larger quantities of the photoproducts.

EXPERIMENTAL SECTION

Materials. Carbon nanopowder (purity >99%) was purchased from Sigma-Aldrich, bis(3-aminopropyl)-terminated oligomeric poly(ethylene glycol) of average molecular weight ~1500 (PEG_{1500N}) was purchased from Anvia Chemicals, CO_2 gas (purity >99.5%) was purchased from Airgas, and hydrogen tetrachloroaurate ($HAuCl_4 \cdot 3H_2O$) and sodium hydroxide (NaOH) were purchased from Alfa-Aesar. Imidazole and fumaric acid were obtained from Aldrich Chemicals, thionyl chloride (purity >99%) was obtained from Alfa Aesar, nitric acid was obtained from VWR, and ^{13}C-enriched sodium bicarbonate ($NaH^{13}CO_3$, purity 97% and ^{13}C content 99%) and D_2O were obtained from Cambridge Isotope Laboratories. HPLC-grade solvents isopropanol, methanol, and phosphoric acid were supplied by Fisher Scientific, and dialysis membrane tubing (MWCO ~500) was supplied by Spectrum Laboratories. Water was deionized and purified by being passed through a Labconco WaterPros water purification system.

Measurements. A Baxter Megafuge (model 2630), Eppendorf (model 5417 R), and Beckman-Coulter ultracentrifuge (Optima L90K with a type 90 Ti fixed-angle rotor) were used for centrifugation at various *g* values. Optical absorption spectra were recorded on a Shimadzu UV-2501PC spectrophotometer. NMR measurements were carried out on Bruker (500 and 300 MHz) and JEOL (500 MHz) NMR spectrometers. GC-MS analyses were performed on a Shimadzu GC-MS instrument (model QP 2010) with an Rxi-XLB/or Rtx-5MS column and an electron ionization (EI) MS detector. Transmission electron microscopy (TEM) images were obtained on Hitachi 9500 TEM and HD-2000 scanning-TEM systems.

Photocatalysts. In the synthesis of PEG_{1500N}-functionalized carbon dots, an as-supplied carbon nanopowder sample (1 g) was refluxed in an aqueous nitric acid solution (5 M, 90 mL) for 48 h. The reaction mixture back at room temperature was dialyzed against fresh water and then centrifuged at 3000*g* to retain the supernatant. The recovered sample containing primarily small carbon nanoparticles was refluxed in neat thionyl chloride for 12 h, followed by the removal of excess thionyl chloride under nitrogen. The post-treatment carbon particle sample (100 mg) was mixed well with carefully dried PEG_{1500N} (1 g) in a flask, heated to 140 °C, and stirred at constant temperature under nitrogen for 72 h. The reaction mixture was cooled to room temperature, dispersed in water, and then centrifuged at 20 000*g* to retain the dark supernatant as an aqueous solution of the as-prepared carbon dots.

For the metal doping of carbon dots, an aqueous dispersion of the carbon dots was mixed with an aqueous solution of gold compound ($HAuCl_4$), and the mixture was irradiated with visible light. The doping level was monitored in terms of the gold plasmon absorption band.[36,37]

Photocatalytic Reactions. The CO_2 photocatalytic reduction experiments under different CO_2 pressures were performed on a setup consisting of a 1 kW xenon arc source coupled with a "hot filter" to eliminate both infrared and UV radiation (transparent only in the 405−720 nm spectral region). Two stainless steel cylindrical optical cells with flat fronts and back sapphire windows (2.5 cm in diameter, sealed with teflon O-rings) were used as photochemical reactors with a pressure limit of at least 2000 psia.[28] The short-path cell had an optical path length of 16 mm (~4 mL in reactor volume), and the long-path cell, 80 mm (~20 mL in reactor volume). In a typical experiment, the cell was first loaded (not completely full) with an aqueous dispersion of the photocatalysts, purged with high-purity nitrogen gas under ambient condition, and then sealed. Pressurized CO_2 (in a syringe pump) was introduced into the sealed cell through the metal tubing and valve until the desired pressure in the cell was achieved, and the actual pressure upon stabilization of the system was measured and recorded by using a precision pressure gauge (Heise).

Some CO_2 photocatalytic reduction experiments under ambient pressure were carried out by using an ACE Glass immersion-well photochemistry apparatus equipped with a 450 W medium-pressure Hanovia lamp coupled with a cycling water filter and a glass or solution filter. An aqueous dispersion of the photocatalysts in the photochemistry apparatus was purged first with high-purity nitrogen gas and then with CO_2 gas (for about 60 min) for saturation, followed by photoirradiation.

Aqueous $NaHCO_3$ or $NaH^{13}CO_3$ solution (up to 80 mM, mimicking mildly acidic conditions of pH ~4.5−5.5) was used as CO_2 or ^{13}C-enriched CO_2 in the same photocatalytic reactions.

Isopropanol was added in some of the experiments described above as a sacrificial electron donor, though no meaningful difference was found in the outcome of the photocatalytic reduction (probably due to the fact that PEG molecules of similar structural elements to those in isopropanol were already in the reaction system).

Photoproduct Characterization and Analysis. The aqueous reaction mixture post-photoirradiation was collected via slow depressurization from the high-pressure optical cell into a cooled flask, followed by short-path distillation into an aqueous NaOH solution (pH ~11) for the organic acids in the reaction mixture to be trapped as salts. Upon the removal of water via evaporation, the resulting solid sample was characterized by using NMR and GC-MS methods. Formic acid and acetic acid (or formate and acetate in some measurements) were identified, confirmed, and quantified. Imidazole and fumaric acid were used as internal standards in the ^1H NMR quantification measurements.

AUTHOR INFORMATION

Corresponding Authors

*E-mail: christopher.bunker@wpafb.af.mil.

*E-mail: syaping@clemson.edu.

Notes

The authors declare no competing financial interest.

ACKNOWLEDGMENTS

This work was made possible by the support of the Air Force Research Laboratory through the nanoenergetics program. Additional support from NSF (Y.-P.S.) and AFOSR (C.E.B.) is also acknowledged.

REFERENCES

(1) Roy, S. C.; Varghese, O. K.; Paulose, M.; Grimes, C. A. Toward Solar Fuels: Photocatalytic Conversion of Carbon Dioxide to Hydrocarbons. *ACS Nano* **2010**, *4*, 1259−1278.

(2) Izumi, Y. Recent Advances in the Photocatalytic Conversion of Carbon Dioxide to Fuels with Water and/or Hydrogen Using Solar Energy and Beyond. *Coord. Chem. Rev.* **2013**, *257*, 171−186.

(3) Dhakshinamoorthy, A.; Navalon, S.; Corma, A.; Garcia, H. Photocatalytic CO_2 Reduction by TiO_2 and Related Titanium Containing Solids. *Energy Environ. Sci.* **2012**, *5*, 9217−9233.

(4) Habisreutinger, S. N.; Schmidt-Mende, L.; Stolarczyk, J. K. Photocatalytic Reduction of CO_2 on TiO_2 and Other Semiconductors. *Angew. Chem., Int. Ed.* **2013**, *52*, 7372−7408.

(5) Feng, X.; Sloppy, J. D.; LaTempa, T. J.; Paulose, M.; Komarneni, S.; Bao, N.; Grimes, C. A. Synthesis and Deposition of Ultrafine Pt Nanoparticles within High Aspect Ratio TiO_2 Nanotube Arrays: Application to the Photocatalytic Reduction of Carbon Dioxide. *J. Mater. Chem.* **2011**, *21*, 13429−13433.

(6) Woolerton, T. W.; Sheard, S.; Pierce, E.; Ragsdale, S. W.; Armstrong, F. A. CO_2 Photoreduction at Enzyme-modified Metal Oxide Nanoparticles. *Energy Environ. Sci.* **2011**, *4*, 2393−2399.

(7) Abou Asi, M.; He, C.; Su, M.; Xia, D.; Lin, L.; Deng, H.; Xiong, Y.; Qiu, R.; Li, X.-Z. Photocatalytic Reduction of CO_2 to Hydrocarbons Using $AgBr/TiO_2$ Nanocomposites under Visible Light. *Catal. Today* **2011**, *175*, 256−263.

(8) Sun, Y.-P.; Zhou, B.; Lin, Y.; Wang, W.; Fernando, K. A. S.; Pathak, P.; Meziani, M. J.; Harruff, B. A.; Wang, X.; Wang, H.; Luo, P. G.; Yang, H.; Kose, M. E.; Chen, B.; Veca, L. M.; Xie, S.-Y. Quantum-

sized Carbon Dots for Bright and Colorful Photoluminescence. *J. Am. Chem. Soc.* **2006**, *128*, 7756−7757.
(9) Cao, L.; Meziani, M. J.; Sahu, S.; Sun, Y.-P. Photoluminescence Properties of Graphene versus Other Carbon Nanomaterials. *Acc. Chem. Res.* **2013**, *46*, 171−180.
(10) Cao, L.; Sahu, S.; Anilkumar, P.; Bunker, C. E.; Xu, J. A.; Fernando, K. A. S.; Wang, P.; Guliants, E. A.; Tackett, K. N., II; Sun, Y.-P. Carbon Nanoparticles as Visible-Light Photocatalysts for Efficient CO_2 Conversion and Beyond. *J. Am. Chem. Soc.* **2011**, *133*, 4754−4757.
(11) Wang, X.; Cao, L.; Lu, F.; Meziani, M. J.; Li, H.; Qi, G.; Zhou, B.; Harruff, B. A.; Kermarrec, F.; Sun, Y.-P. Photoinduced Electron Transfers with Carbon Dots. *Chem. Commun.* **2009**, 3774−3776.
(12) Moon, G.-H.; Kim, H.-I.; Shin, Y.; Choi, W. Chemical-Free Growth of Metal Nanoparticles on Graphene Oxide Sheets under Visible Light Irradiation. *RSC Adv.* **2012**, *2*, 2205−2207.
(13) Qin, X.; Lu, W.; Asiri, A. M.; Al-Youbi, A. O.; Sun, X. Green, Low-Cost Synthesis of Photoluminescent Carbon Dots by Hydrothermal Treatment of Willow Bark and Their Application as an Effective Photocatalyst for Fabricating Au Nanoparticles−Reduced Graphene Oxide Nanocomposites for Glucose Detection. *Catal. Sci. Technol.* **2013**, *3*, 1027−1035.
(14) Liu, R.; Huang, H.; Li, H.; Liu, Y.; Zhong, J.; Li, Y.; Zhang, S.; Kang, Z. Metal Nanoparticle/Carbon Quantum Dot Composite as a Photocatalyst for High-Efficiency Cyclohexane Oxidation. *ACS Catal.* **2014**, *4*, 328−336.
(15) Hong, J.; Zhang, W.; Ren, J.; Xu, R. Photocatalytic Reduction of CO_2: A Brief Review on Product Analysis and Systematic Methods. *Anal. Methods* **2013**, *5*, 1086−1097.
(16) Wang, X.; Cao, L.; Yang, S.-T.; Lu, F.; Meziani, M. J.; Tian, L.; Sun, K. W.; Bloodgood, M. A.; Sun, Y.-P. Bandgap-Like Strong Fluorescence in Functionalized Carbon Nanoparticles. *Angew. Chem., Int. Ed.* **2010**, *49*, 5310−5314.
(17) Xu, J.; Sahu, S.; Cao, L.; Bunker, C. E.; Peng, G.; Liu, Y.; Fernando, K. A. S.; Wang, P.; Guliants, E. A.; Meziani, M. J.; Qian, H.; Sun, Y.-P. Efficient Fluorescence Quenching in Carbon Dots by Surface-Doped Metals-Disruption of Excited State Redox Processes and Mechanistic Implications. *Langmuir* **2012**, *28*, 16141−16147.
(18) Qin, X.; Lu, W.; Chang, G.; Luo, Y.; Asiri, A.; Al-Youbi, A.; Sun, X. Novel Synthesis of Au Nanoparticles Using Fluorescent Carbon Nitride Dots as Photocatalyst. *Gold Bull.* **2012**, *45*, 61−67.
(19) Bikkina, P. K.; Shoham, O.; Uppaluri, R. Equilibrated Interfacial Tension Data of the CO_2-Water System at High Pressures and Moderate Temperatures. *J. Chem. Eng. Data* **2011**, *56*, 3725−3733.
(20) Goren, Z.; Willner, I.; Nelson, A. J.; Frank, A. J. Selective Photoreduction of Carbon Dioxide/Bicarbonate to Formate by Aqueous Suspensions and Colloids of Palladium-Titania. *J. Phys. Chem.* **1990**, *94*, 3784−3790.
(21) Johne, P.; Kisch, H. Photoreduction of Carbon Dioxide Catalysed by Free and Supported Zinc and Cadmium Sulphide Powders. *J. Photochem. Photobiol., A: Chem.* **1997**, *111*, 223−228.
(22) Zhao, Z. H.; Fan, J. M.; Xie, M. M.; Wang, Z. Z. Photo-catalytic Reduction of Carbon Dioxide with in-situ Synthesized CoPc/TiO_2 under Visible Light Irradiation. *J. Clean Prod.* **2009**, *17*, 1025−1029.
(23) Sato, S.; Arai, T.; Morikawa, T.; Uemura, K.; Suzuki, T. M.; Tanaka, H.; Kajino, T. Selective CO_2 Conversion to Formate Conjugated with H_2O Oxidation Utilizing Semiconductor/Complex Hybrid Photocatalysts. *J. Am. Chem. Soc.* **2011**, *133*, 15240−15243.
(24) Yadav, R. K.; Baeg, J.-O.; Oh, G. H.; Park, N.-J.; Kong, K.-j.; Kim, J.; Hwang, D. W.; Biswas, S. K. A Photocatalyst-Enzyme Coupled Artificial Photosynthesis System for Solar Energy in Production of Formic Acid from CO_2. *J. Am. Chem. Soc.* **2012**, *134*, 11455−11461.
(25) Eggins, B. R.; Irvine, J. T. S.; Murphy, E. P.; Grimshaw, J. Formation of Two-carbon Acids from Carbon Dioxide by Photoreduction on Cadmium Sulphide. *J. Chem. Soc., Chem. Commun.* **1988**, 1123−1124.
(26) Irvine, J. T. S.; Eggins, B. R.; Grimshaw, J. Solar Energy Fixation of Carbon Dioxide via Cadmium Sulphide and Other Semiconductor Photocatalysts. *Sol. Energy* **1990**, *45*, 27−33.
(27) Ishitani, O.; Inoue, C.; Suzuki, Y.; Ibusuki, T. Photocatalytic Reduction of Carbon Dioxide to Methane and Acetic Acid by an Aqueous Suspension of Metal-deposited TiO_2. *J. Photochem. Photobiol., A: Chem.* **1993**, *72*, 269−271.
(28) Pathak, P.; Meziani, M. J.; Li, Y.; Cureton, L. T.; Sun, Y.-P. Improving Photoreduction of CO_2 with Homogeneously Dispersed Nanoscale TiO_2 catalysts. *Chem. Commun.* **2004**, 1234−1235.
(29) Srinivas, B.; Shubhamangala, B.; Lalitha, K.; Reddy, P. A. K.; Kumari, V. D.; Subrahmanyam, M.; De, B. R. Photocatalytic Reduction of CO_2 over Cu-TiO_2/Molecular Sieve 5A Composite. *Photochem. Photobiol.* **2011**, *87*, 995−1001.
(30) Hoffmann, M. R.; Moss, J. A.; Baum, M. M. Artificial Photosynthesis: Semiconductor Photocatalytic Fixation of CO_2 to Afford Higher Organic Compounds. *Dalton Trans.* **2011**, *40*, 5151−5158.
(31) Fox, M. A.; Dulay, M. T. Heterogeneous Photocatalysis. *Chem. Rev.* **1993**, *93*, 341−357.
(32) Shkrob, I. A.; Marin, T. W.; He, H.; Zapol, P. Photoredox Reactions and the Catalytic Cycle for Carbon Dioxide Fixation and Methanogenesis on Metal Oxides. *J. Phys. Chem. C* **2012**, *116*, 9450−9460.
(33) Maeda, K.; Eguchi, M.; Youngblood, W. J.; Mallouk, T. E. Niobium Oxide Nanoscrolls as Building Blocks for Dye-Sensitized Hydrogen Production from Water under Visible Light Irradiation. *Chem. Mater.* **2008**, *20*, 6770−6778.
(34) Maeda, K.; Eguchi, M.; Lee, S.-H. A.; Youngblood, W. J.; Hata, H.; Mallouk, T. E. Photocatalytic Hydrogen Evolution from Hexaniobate Nanoscrolls and Calcium Niobate Nanosheets Sensitized by Ruthenium(Ii) Bipyridyl Complexes. *J. Phys. Chem. C* **2009**, *113*, 7962−7969.
(35) Wang, J.; Sahu, S.; Sonkar, S. K.; Tackett, K. N., II; Sun, K. W.; Liu, Y.; Maimaiti, H.; Anilkumar, P.; Sun, Y.-P. Versatility with Carbon Dots-from Overcooked BBQ to Brightly Fluorescent Agents and Photocatalysts. *RSC Adv.* **2013**, *3*, 15604−15607.
(36) Jain, P. K.; Lee, K. S.; El-Sayed, I. H.; El-Sayed, M. A. Calculated Absorption and Scattering Properties of Gold Nanoparticles of Different Size, Shape, and Composition: Applications in Biological Imaging and Biomedicine. *J. Phys. Chem. B* **2006**, *110*, 7238−7248.
(37) Liu, X.; Atwater, M.; Wang, J.; Huo, Q. Extinction Coefficient of Gold Nanoparticles with Different Sizes and Different Capping Ligands. *Colloids Surf., B* **2007**, *58*, 3−7.